

Original Research

CoQ10 Improves Myocardial Damage in Doxorubicin-Induced Heart Failure in C57BL/6 Mice

Zuowei Pei^{1,2,†}, Liang Ma^{1,†}, Yawen Li¹, Jin Yang², Qin Yang³, Wei Yao³, Shijun Li^{1,*}

¹Department of Cardiology, Central Hospital of Dalian University of Technology, 116033 Dalian, Liaoning, China

²Department of Central Laboratory, Central Hospital of Dalian University of Technology, 116033 Dalian, Liaoning, China

³Department of Internal Medicine, Affiliated Zhong Shan Hospital of Dalian University, 116001 Dalian, Liaoning, China

*Correspondence: lshijun@126.com (Shijun Li)

†These authors contributed equally.

Academic Editor: Iain Hargreaves

Submitted: 19 May 2022 Revised: 1 July 2022 Accepted: 21 July 2022 Published: 15 August 2022

Abstract

Background: Cardiovascular disease is associated with high morbidity and mortality. Doxorubicin (DOX) is an effective adjunct to cancer chemotherapy but leads to cardiovascular-related side effects. Because coenzyme Q10 (CoQ10) has been shown to protect against cardiac damage, this study was conducted to investigate the protective effects of CoQ10 against cardiac damage in mice. **Methods:** We randomly divided six-week-old male C57BL/6 mice into four groups: control (n = 7), CoQ10 (n = 7), heart failure (HF) (n = 7), and HF+CoQ10 (n = 6) groups. HF group was induced via intraperitoneal injections with DOX (5 mg/kg) once weekly for 4 weeks. CoQ10 was soluble in corn oil. The mice of CoQ10 and HF+CoQ10 group were given CoQ10 (100 mg/kg) once a day for 8 weeks. All mice were subjected to different treatment regimens for eight weeks. Metabolic characteristics, cardiac damage, oxidative stress markers (SIRT1, SIRT3, eNOS, TE, P53, SIRT5, CAT, HO-1, and SOD), energy metabolism markers (PARP-1 and PPAR- γ), myocardial fibrosis markers (Smad3 and TGF- β), and apoptosis markers (BAK, BCL-XL, and caspase-8) were analyzed at eight weeks after the different treatments. **Results:** CoQ10 reduced the levels of molecules related to cardiac damage, oxidative stress, energy metabolism, and myocardial fibrosis in mice with doxorubicin-induced HF. CoQ10 also exerted anti-apoptotic effects in HF mice. **Conclusions:** CoQ10 may be useful for preventing cardiac damage in DOX-induced HF.

Keywords: heart failure; coenzyme Q10; doxorubicin; cardiac damage

1. Introduction

The American Heart Association/American College of Cardiology guidelines define heart failure (HF) as “a complex clinical syndrome that can result from any structural or functional cardiac disorder that impairs the ability of the ventricle to fill or eject blood” [1]. HF is a global epidemic disease; although many treatments for HF have been developed in recent years, the mortality rate remains high [2].

The deaths of cancer survivors are typically attributable to cardiac-related factors [3]. Doxorubicin (DOX) belongs to the anthracycline class of drugs and is widely used in chemotherapy for various cancers, such as stomach cancer, breast cancer, and lung cancer [4,5]. DOX causes cardiotoxicity as a side effect and is widely used in animal studies to induce HF [6,7]. Oxidative stress, lipid peroxidation, apoptosis, and autophagy disorders are thought to be major factors associated with DOX-induced cardiotoxicity [7–9]. HF is an important cause of high mortality, high morbidity, and poor quality of life. However, drugs that can reduce the cardiotoxicity of DOX are lacking.

CoQ10 is a major cofactor involved in oxidative phosphorylation in mitochondria [10]. CoQ10, one of the syn-

thetic antioxidants in the body, was the first drug used to improve mortality related to cardiac disease, reducing deaths by 50% [11]. CoQ10, which exists in oxidized ubiquinone and reduced ubiquinol forms, is produced in various tissues, most commonly the cardiac, kidney, liver, and muscle tissues [12]. CoQ, an intermediate state of CoQ oxidation “ubisemiquinone”, is also ubiquitous and present in all tissues that have mitochondria [13]. CoQ10 is safe for treating cardiac failure and reducing major adverse cardiovascular events [14]. Furthermore, Khan *et al.* [15] found that CoQ10 protects the cardiac tissue of apoptotic mice by downregulating apoptosis-related genes. Additionally, CoQ10 relieves cardiac damage caused by hyperlipidemia [16]. It is consistent with the beneficial effects of other natural compounds such as quercetin and ascorbic acid and has great potential as a heart protectant in cancer patients [17]. However, the mechanism by which CoQ10 attenuates DOX-induced cardiotoxicity is unclear.

This study was conducted to determine the effect of CoQ10 on DOX-induced cardiac damage. Our findings improve the understanding of the mechanism and effect of CoQ10 in DOX-induced HF.



2. Materials and Methods

Six-week-old male C57BL/6 mice were purchased from Liaoning Changsheng biotechnology CO, LTD (Liaoning, China) and mice were allowed to adapt to one week. All mice were randomly divided into four groups as follows: a control group ($n = 7$), a HF group ($n = 7$), a CoQ10 group ($n = 7$), a HF+CoQ10 group ($n = 6$). Four groups mice were housed in a room under diurnal lighting conditions with a controlled temperature (24°C). HF group was induced via intraperitoneal injections with DOX (5 mg/kg) once weekly for 4 weeks. CoQ10 was soluble in corn oil. The mice of CoQ10 and HF+CoQ10 group were given CoQ10 (100 mg/kg) once a day for 8 weeks [18]. Mice in all groups were fed the appropriate diet for eight weeks. Blood samples were acquired from eyeball blood in serum tubes and stored at -80°C until use. Heart tissues were fixed in 10% formalin and embedded in paraffin for histological evaluation. The remaining heart tissues were snap-frozen in liquid nitrogen for Real-Time Reverse Transcription Polymerase Chain Reaction (PCR) or Western blot analysis. All animal experiments were performed in accordance with the Guide for the Care and Use of Laboratory Animals and approved by the Ethics Committee of Dalian Municipal Central Hospital.

2.1 Biochemical Measurements

Blood samples were collected, and serum was prepared by centrifugation at 2500 g for 5 min, after which the supernatant was collected and used for lactate dehydrogenase (LDH) and creatine kinase MB (CK-MB) measurements using commercially available kits according to the manufacturer's instructions (Nanjing Jiancheng Bioengineering Institute, Nanjing, China).

2.2 Histological Measurements

Heart tissue was immersed in 1:9 mg/ μL normal saline to obtain homogenate, and centrifuged at 715 g for 20 min. N-terminal B-type natriuretic peptide (NT-proBNP), Telomerase (TE), SIRT1, SIRT3, and endothelial nitric oxide synthase (eNOS) were then measured using supernatant using commercially available kits according to the manufacturer's instructions (Jiangsu Meibiao Biotechnology Co., Ltd., Jiangsu, China).

2.3 Histological Staining

Mice were anesthetized with isoflurane (1.5%) at the beginning, when hearts were fixed by perfusion with 10% buffered formalin and used isoflurane (4%) via a nozzle placed over the nose. The hearts were fixed overnight at room temperature, transferred into 70% ethanol, and then embedded in paraffin. Paraffin-embedded heart tissue slices were deparaffinized via immersion in xylene (three times, 5 min each) rehydrated in a descending alcohol series (100%, 90%, 80%, and 70% alcohol, 5 min each). Histological changes were detected by staining 5- μm -thick

sections with hematoxylin and eosin (HE) stain, Masson's trichrome stain, and FITC-conjugated wheat germ agglutinin (WGA) stain using the HE staining kit (G1120; Beijing Solarbio Science & Technology Co., Ltd.), Masson staining kit (G1340; Beijing Solarbio Science & Technology Co., Ltd.) and WGA staining kit (L4895; Sigma-Aldrich, St. Louis, MO, USA). Images were acquired microscopically using a $B \times 40$ upright light microscope (Olympus, Tokyo, Japan).

2.4 Assessment of Apoptosis by TUNEL Staining

The hearts were embedded in paraffin, and serially sectioned to 5 μm thickness. The sections were deparaffinized and hydrated in xylene and gradient concentrations of ethanol, and then incubated in proteinase K (37°C , 22 min) and stained using the Fluorescein TUNEL Cell Apoptosis Detection kit (Servicebio Technology Co., Ltd., Wuhan, China). The images were captured using a fluorescence microscope (Nikon, Japan). Cells that were positive for TUNEL staining and aligned with DAPI staining were considered apoptotic cells and counted.

2.5 Immunohistochemistry Analysis (IHC)

Coronal sections of the heart tissues were fixed in 10% formalin, dehydrated in an ascending series of ethanol, and embedded in paraffin for histological evaluation. For immunohistochemical staining, the heart sections were deparaffinized and rehydrated. Next, the sections were blocked with 3% H_2O_2 in methanol for 15 min to inactivate endogenous peroxidases and then incubated overnight at 4°C with one of the following primary antibodies: BNP (rabbit anti-NPPB polyclonal antibody, 1:100; Solarbio, Beijing, China); SIRT3 (Rabbit Anti-SIRT3 Polyclonal antibody, 1:50; Solarbio); HO-1 (Rabbit Anti-HMOX-1 antibody, 1:100; Solarbio); SOD (Anti-SOD1 Polyclonal antibody, 1:100; Solarbio); PARP-1 (Anti-PARP1 Rabbit mAb, 1:50; PTM BIO, Hangzhou, China); PPAR- γ (PPAR Gamma Rabbit Polyclonal antibody, 1:200; Proteintech); SMAD3 (Anti-Phospho-Smad2-S465/467+Smad3-S423/425, 1:200; Solarbio); TGF- β (Rabbit Anti-TGF- β Polyclonal antibody, 1:300; Solarbio); interleukin (IL)-1 β (rabbit anti-IL-1 β polyclonal antibody, 1:100; Proteintech); IL-6 (rabbit anti-IL-6 polyclonal antibody, 1:100; Proteintech); IL-10 (rabbit anti-IL-10 polyclonal antibody, 1:100; Proteintech); BCL-XL (Rabbit Anti-BCL-XL Polyclonal antibody, 1:100; Solarbio); BAK (Anti-BAK1 Polyclonal Antibody, 1:100; Solarbio); Caspase8 (Anti-Caspase-8 Rabbit mAb, 1:50; PTM BIO). The sections were then incubated for 30 min at room temperature with a goat anti-rabbit HRP secondary antibody (antirabbit/rabbit Universal Immunohistochemical Detection Kit; Proteintech). All sections were examined with an Olympus $B \times 40$ upright light microscope (Olympus, Tokyo, Japan).

2.6 Western Blot Analysis

Proteins were extracted using radioimmunoprecipitation assay buffer (P0013B; Beyotime, Shanghai, China). Protein samples were first separated by 10% sodium dodecyl sulfate-polyacrylamide gel electrophoresis (SDS-PAGE), and then transferred to polyvinylidene fluoride membranes (Immobilon, Millipore, Billerica, MA, USA). The membranes were blocked with 5% skim milk in TBST buffer (TBS containing 0.1% Tween-20) at room temperature for 1 h, and then incubated with one of the following primary antibodies at 4 °C overnight: PARP-1 (Anti-PARP1 Rabbit mAb, 1:500; PTM BIO); PPAR- γ (PPAR Gamma Rabbit Polyclonal antibody, 1:2000; Proteintech); The immunoreactive proteins were quantified using NIH ImageJ software. GAPDH (GAPDH Polyclonal antibody, 1:2000; Proteintech) was used as an internal control. The protein levels are expressed as protein/GAPDH ratios.

2.7 RNA Isolation and Real-Time PCR (qPCR)

Total RNA was isolated from heart tissues and complementary DNA (cDNA) was synthesized using the TransScript One-Step gDNA Removal and cDNA Synthesis SuperMix kit according to the manufacturer's protocol. Gene expression was quantitatively analyzed using qPCR and the TransStart Top Green qPCR SuperMix kit (SuperScript VILO cDNA synthesis kit; Thermo Fisher Scientific, Inc.). The specific gene expression levels were quantitatively analyzed by performing qPCR using fluorescent SYBR Green technology (Light Cycler; Roche Molecular Diagnostics). β -actin cDNA was amplified and quantified in each cDNA preparation to normalize the relative expression of target genes. The thermocycling conditions were as follows: 95 °C for 3 min; 95 °C for 15 sec; 60 °C for 15 sec; 72 °C for 1 min (35 cycles); and 72 °C for 10 min. GAPDH was amplified and quantitated in each reaction to normalize the relative amounts of the target genes. Primer sequences are listed in Table 1.

Table 1. Primer oligonucleotide sequences.

Gene	Primers
GAPDH	F: 5'-CCTCGTCCCGTAGACAAAATG-3'
	R: 5'-TGAGGTCAATGAAGGGGTCGT-3'
P53	F: 5'-CCCTCTGAGCCAGGAGACATT-3'
	R: 5'-CCCAGGTGGAAGCCATAGTTG-3'
SIRT5	F: 5'-GTGTTGTAGACGAAAGCCTCCTG-3'
	R: 5'-TCCAGTAACCTCCAGCGCCT-3'
CAT	F: 5'-CCAGCGACCAGATGAAGCAG-3'
	R: 5'-GTGACCTCAAAGTATCCAAAAGCA-3'

2.8 Statistical Analysis

All data are presented as mean \pm SEM. The statistical analysis was performed using SPSS version 23.0 (SPSS Inc., Chicago, IL, USA). The data was tested for normality. Inter-group variation was measured by one-way analysis of variance and a subsequent Tukey's test. The minimal level for significance was $p < 0.05$.

3. Results

3.1 Metabolic Characterization

The metabolic characteristics of the mice subjected to the different treatments are summarized in Fig. 1. The heart/body weight ratio did not significantly ($p > 0.05$) differ among the four groups (Fig. 1A). Mice in the HF group showed considerably increased serum NT-proBNP, LDH, and CK-MB levels, whereas the levels of these proteins were significantly decreased in the HF+CoQ10 group ($p < 0.01$) (Fig. 1B). Compared with the HF group, the HF+CoQ10 group showed significantly decreased expression of BNP in IHC staining performed to evaluate the expression levels of BNP ($p < 0.01$) (Fig. 1C,D).

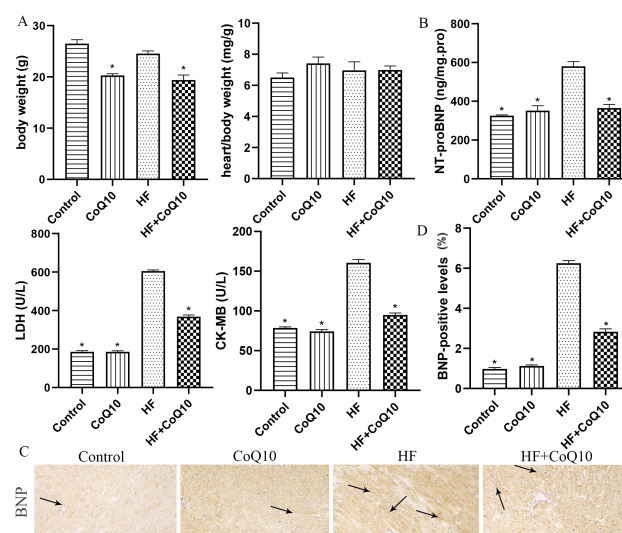


Fig. 1. Metabolic data in different groups after treatment with CoQ10. (A) Quantitative analysis of heart/body weight in different groups. Data are shown as the means \pm SEM. $n = 6-7$ per group. (B) LDH, CK-MB, and NT-proBNP levels in the different groups. Data are shown as the means \pm SEM. $n = 6-7$ per group. $*p < 0.01$ vs HF group. (C) Representative immunohistochemical staining results for BNP in cardiac tissues. (D) Quantification of positive expression. Magnification 40 \times . The arrows indicate positively stained cells. Data are shown as the means \pm SEM. $n = 3$ per group. $*p < 0.01$ vs HF group. Abbreviations: BNP, bone natriuretic protein; CK-MB, creatinine kinase-MB; CoQ10, coenzyme Q10; HF, heart failure; LDH, lactate dehydrogenase; NT-proBNP, pro-hormone bone natriuretic protein.

3.2 Cardiac Tissue Damage

Wheat-germ agglutinin and hematoxylin and eosin staining revealed cardiomyocyte hypertrophy and inflammatory cell infiltration. Compared with the control group, the HF group exhibited myocardial hypertrophy, as evidenced by an increase in the cross-sectional area of cardiomyocytes (Fig. 2B) and inflammatory cell infiltration (Fig. 2A), both of which were attenuated by CoQ10.

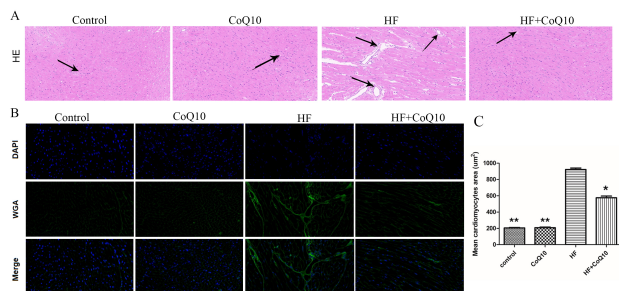


Fig. 2. Cardiac tissue damage in the different groups after the treatment of CoQ10. (A) Effect of CoQ10 on DOX-induced histopathological changes in the cardiac tissues. Histopathological changes were evaluated using HE staining. Arrows indicate positively stained cells. (B) WGA staining for quantitative analysis of cardiomyocyte cross-sectional area. (C) Quantification of positive expression. Data are shown as the means \pm SEM. $n = 3$ per group. $*p < 0.05$ vs HF group; $**p < 0.01$ vs HF group. Abbreviations: CoQ10, coenzyme Q10; DOX, doxorubicin; HE, hematoxylin and eosin; HF, heart failure; WGA, wheat germ agglutinin.

3.3 CoQ10 Repressed DOX-Induced Cardiac Oxidative Stress

The activity of heart biomarkers, such as SIRT1, SIRT3, eNOS, and TE, was significantly decreased in the HF group than control group and increased in the HF+CoQ10 group than HF group ($p < 0.01$) (Fig. 3A). Furthermore, the P53 level was significantly suppressed, whereas SIRT5 and CAT expressions were significantly increased in the HF+CoQ10 group compared with that in the HF group ($p < 0.01$) (Fig. 3B). Immunohistochemistry analysis showed that compared with the HF group, the HF+CoQ10 group exhibited significantly increased expression levels of HO-1, SIRT3, and SOD ($p < 0.01$) (Fig. 3C,D).

3.4 CoQ10 Repressed DOX-Induced Cardiac Energy Metabolism

Western blotting (Fig. 4A,B) and immunohistochemistry (Fig. 4C,D) was performed to evaluate the levels of indicators related to energy metabolism. Compared to in the HF group, the expression levels of PARP-1 and PPAR- γ were decreased in the HF+CoQ10 group ($p < 0.05$).

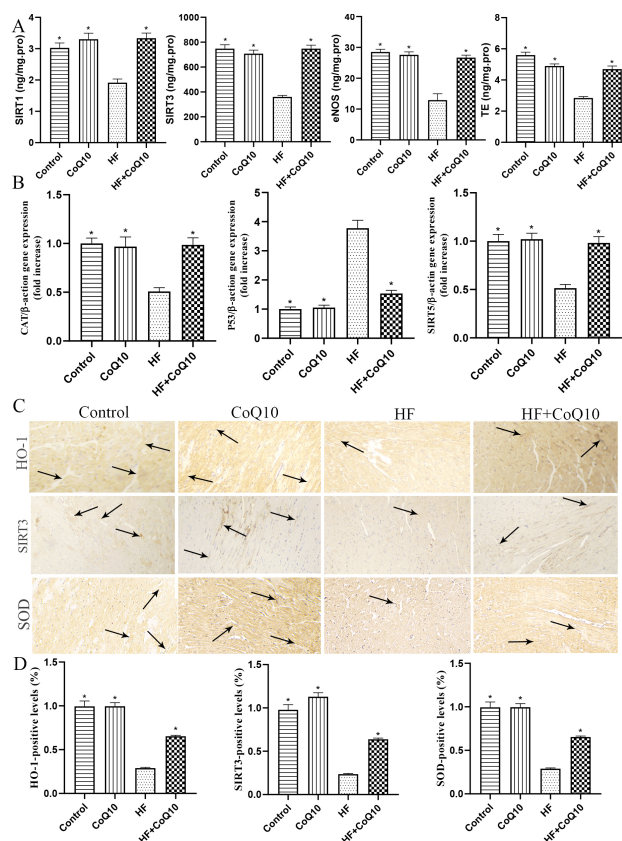


Fig. 3. Cardiac oxidative stress in different groups after treatment with CoQ10. (A) Histological quantification of SIRT1, SIRT3, TE, and eNOS levels. Data are shown as the means \pm SEM. $n = 6-7$ per group. $*p < 0.01$ vs HF group. (B) Bar graph showing P53, CAT, and SIRT5 mRNA expression levels. Data are shown as the means \pm SEM. $n = 6-7$ per group. $*p < 0.01$ vs HF group. (C) Representative immunohistochemistry results for SIRT3, SOD, and HMOX1 in heart tissues. Arrows indicate positively stained cells. (D) Quantification of positive expression. Data are shown as the means \pm SEM. $n = 3$ per group. $*p < 0.01$ vs HF group. Abbreviations: CoQ10, coenzyme Q10; HF, heart failure.

3.5 CoQ10 Repressed DOX-Induced Cardiac Energy Metabolism

Immunohistochemistry (Fig. 5A,B) was performed to evaluate the levels of indicators related to inflammation. The expression levels of IL-1 β and IL-6 were significantly decreased in the HF+CoQ10 group compared to in the HF group ($p < 0.01$). In contrast, the expression of IL-10 was significantly decreased in the HF group and increased in the HF+CoQ10 group ($p < 0.01$).

3.6 CoQ10 Inhibited DOX-Induced Cardiac Fibrosis

To examine cardiac fibrosis in the mice of different treatment groups, Masson and IHC staining was conducted (Fig. 6). The results revealed increased collagen deposition in the HF group compared with control group ($p < 0.01$).

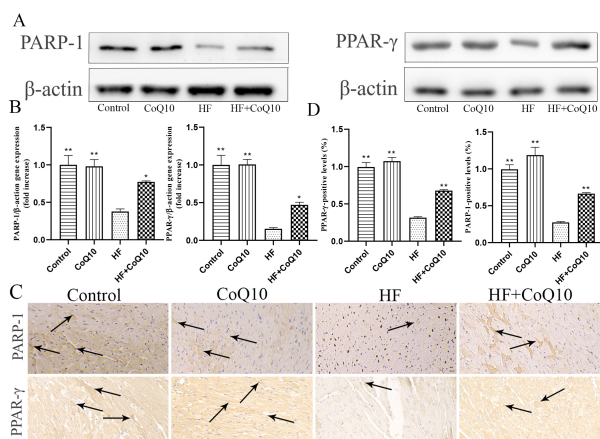


Fig. 4. Cardiac energy metabolism in different groups after treatment with CoQ10. (A) Cardiac PARP-1 and PARP-γ levels assessed using western blotting. (B) Relative protein expression levels. Magnification 40×. Data are presented as the means ± SEM. n = 6–7 per group. * $p < 0.05$ vs HF group; ** $p < 0.01$ vs HF group. (C) Representative immunohistochemistry results for PARP-1 and PARP-γ in cardiac tissues. Arrows indicate positively stained cells. (D) Quantification of positive expression. Data are shown as the means ± SEM. n = 3 per group. ** $p < 0.01$ vs HF group. Abbreviations: CoQ10, coenzyme Q10; HF, heart failure.

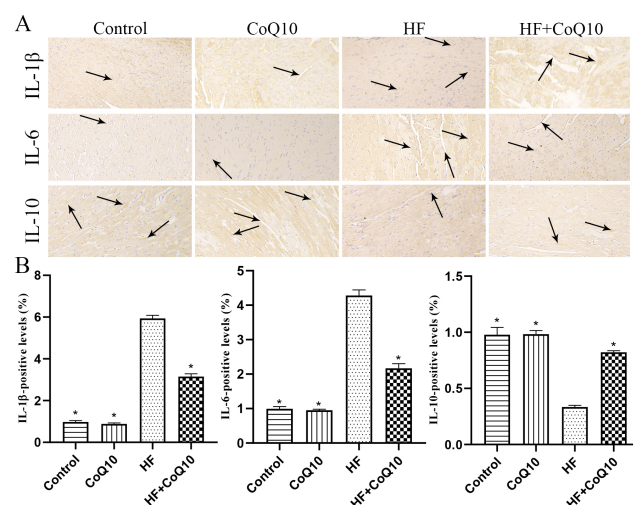


Fig. 5. CoQ10 decreased inflammation in the heart of HF mice. (A) Representative immunohistochemistry images showing the levels of IL-1β, IL-6, and IL-10 in the heart tissues. Arrows indicate positively stained cells. (B) Bar graphs show the levels of IL-1β-, IL-6-, and IL-10-positive cells. Data are presented as the means ± SEM. n = 3 per group. * $p < 0.01$ vs HF group. Abbreviations: CoQ10, coenzyme Q10; HF, heart failure.

(Fig. 6A). However, the expression of SMAD3 and TGF-β was upregulated in the HF group, which was significantly attenuated in the HF+CoQ10 group ($p < 0.01$) (Fig. 6B,C).

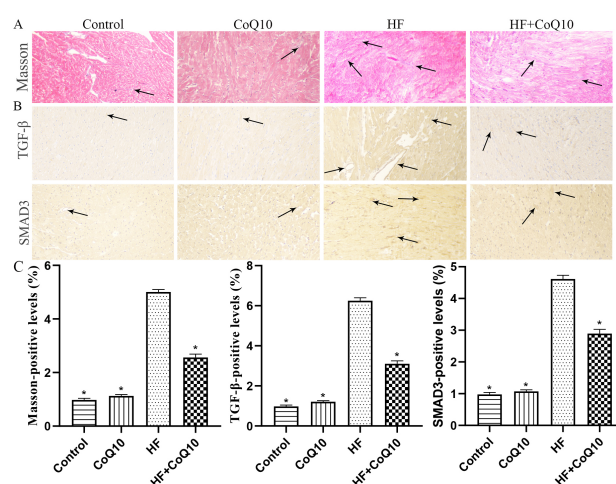


Fig. 6. CoQ10 decreases fibrosis in HF mice. (A) Masson's trichrome staining for collagen deposition in the heart tissue. Arrows indicate positively stained cells. (B) Representative immunohistochemistry results for SMAD3 and TGF-β in the heart tissues. Arrows indicate positively stained cells. (C) Bar graphs show Masson, SMAD3, and TGF-β staining positive levels. Data are shown as the means ± SEM. n = 3 per group. * $p < 0.01$ vs HF group. Abbreviations: CoQ10, coenzyme Q10; HF, heart failure.

3.7 CoQ10 Suppressed DOX-Induced Myocardial Apoptosis

The number of TUNEL-positive cells increased in the hearts of HF group mice compared to in those of control group mice, whereas heart cell apoptosis was reduced in the HF+CoQ10 group (Fig. 7A). Immunoblotting showed that expression of the pro-apoptotic proteins BAK and caspase-8 was significantly increased and that of BCL-XL was decreased in the HF group ($p < 0.01$) (Fig. 7B). CoQ10 treatment reduced the BAK and caspase-8 levels and enhanced the expression of BCL-XL in the HF+CoQ10 group. These results indicate that CoQ10 prevents apoptosis in HF mice.

4. Discussion

Treatment with CoQ10 reduced cardiac damage associated with DOX-induced cardiac failure. Additionally, cardiac dysfunction associated with DOX-induced HF was due to the acceleration of cardiac tissue damage, oxidative stress, myocardial fibrosis, and apoptosis. These findings are summarized in Fig. 8.

DOX is a chemical widely used to treat cancer but has cardiotoxic side effects, resulting in limited use [19]. The mechanism of DOX-induced cardiotoxicity is not completely understood. Furthermore, oxidative stress is considered the core mechanism of HF [20]. Recently, Tadokoro *et al.* [21] showed that ferroptosis is the major form of regulated cell death in DOX-induced cardiotoxicity. Recent studies also confirmed that cardiac fibrosis, apoptosis, coke death, autophagy, and acetylation are closely associated with DOX-induced cardiotoxicity [22–24].

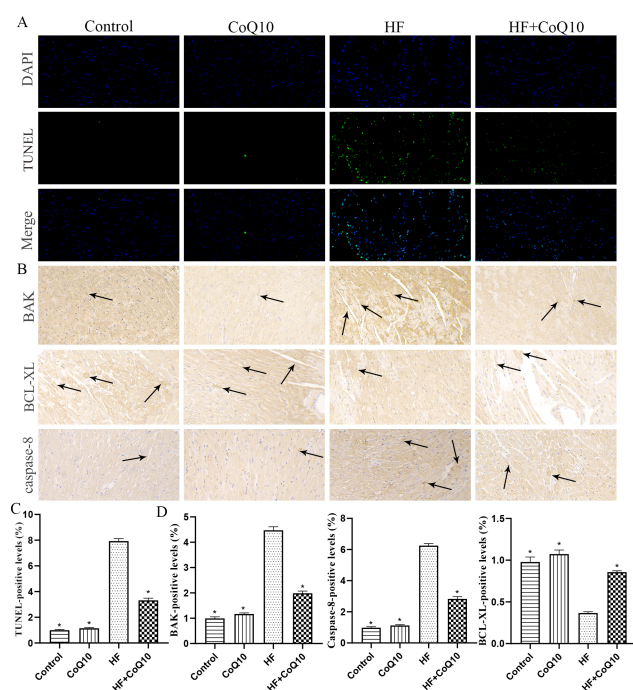


Fig. 7. CoQ10 decreases myocardial apoptosis in HF mice. (A) TUNEL staining (green fluorescence) and DAPI staining (blue fluorescence) photomicrographs to detect apoptosis in the heart tissue. (B) Representative immunohistochemistry results for BAK, caspase-8, and BCL-XL in the heart tissues. Arrows indicate positively stained cells. (C–D) Bar graph shows the positive levels. Data are shown as the means \pm SEM. $n = 3$ per group. $*p < 0.01$ vs HF group. Abbreviations: CoQ10, coenzyme Q10; HF, heart failure.

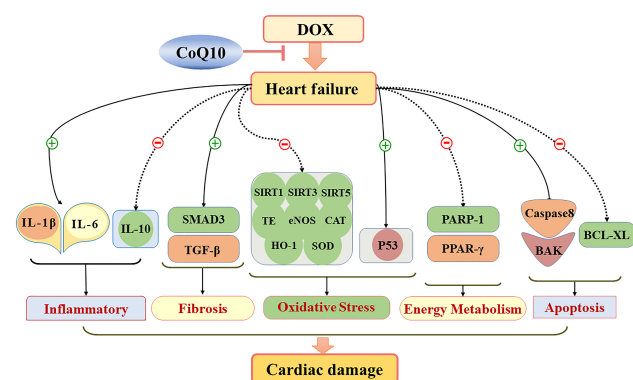


Fig. 8. Schematic diagram showing how CoQ10 protects against cardiac damage in HF mice. CoQ10 regimen prevented cardiac dysfunction and reduced cardiac damage by reducing myocardial oxidative stress, myocardial fibrosis, and apoptosis in HF mice. Abbreviations: CoQ10, coenzyme Q10; HF, heart failure.

CoQ10 is closely related to cardiovascular disease and plays an important role in protecting against these diseases, such as hypertension, hyperlipidemia, myocardial infarction, and HF [13,25–27]. Complementary and integrative

medicine (CIM), such as *G. lucidum* and CoQ10, have a potentially effective role in the treatment of cancer [28]. In addition, CoQ10 influences the effects of adjuvant therapy used for nervous system diseases and tumors [26,29]. However, the mechanism of the protective effect of CoQ10 on DOX-induced HF is unclear.

The metabolic characteristics of NT-proBNP, LDH, and CK-MB showed that our animal models were successfully prepared. HF is characterized by cardiac remodeling. Our results revealed cardiac remodeling and inflammation infiltration similar to those in HF. CoQ10 treatment effectively reduced myocardial remodeling and inflammation infiltration.

Oxidative stress is important in the pathophysiology and pathogenesis of HF and is widely considered a cause of DOX-induced cardiotoxicity [30,31]. CoQ10 is a co-factor of oxidative phosphorylation in the mitochondria, which are crucial for cellular energy production. Therefore, CoQ10 is closely associated with oxidative stress and has a high antioxidant capacity [13]. SIRT3 is a major mitochondrial deacetylase that participates in antioxidant oxidation by regulating the acetylation of antioxidant enzymes [32]. Previous studies showed that SIRT3 regulates various types of antioxidants. Moreover, a study confirmed that SIRT3 is involved in p53-mediated ferroptosis and that Sirt3 and P53 play key roles in oxidative stress [33]. The endogenous antioxidant HO-1 may be a target molecule for treating antioxidant stress injury in HF [34]. CoQ10 improved lipid peroxidation by decreasing malondialdehyde levels in human cardiac cells [35]. In the present study, HF down-regulated the expression of SIRT3 and HO-1 in myocardial tissues, whereas treatment with CoQ10 increase their expression. The levels of SIRT1, SIRT3, SIRT5, eNOS, TE, CAT, and P53 were significantly downregulated in the HF mouse heart, and these levels were restored by CoQ10.

PPAR- γ is important in the progression of HF [36]. PPAR-1 and PPAR- γ are transcription factors that promote antioxidant pathways in the endothelium [37]. In the present study, CoQ10 reversed the heart energy metabolism of PPAR-1 and PPAR- γ in HF mice and exerted a protective role in DOX-induced heart injury.

Anthracyclines cause severe cellular inflammation that leads to cell death [38]. IL-1 β and IL-6 are typical pro-inflammatory cytokines, whereas IL-10 is an anti-inflammatory molecule [39]. CoQ10 has been shown to decrease the release of pro-inflammatory factors and increase the release of anti-inflammatory factors, which is important in fighting inflammation [40]. Also, our result indicated that CoQ10 reduce inflammation in cardiac caused by DOX.

Myocardial fibrosis is central to the pathology of HF. CoQ10 may protect against lung fibroblast formation and alleviate fibrosis by inhibiting TGF- β [41]. However, whether CoQ10 can inhibit cardiac fibrosis in mice was unclear. Our results suggest that CoQ10 reduced cardiac fi-

brosis by inhibiting TGF- β and SMAD3.

Apoptosis is a form of cell death mediated by caspases. Inhibition of myocardial apoptosis can effectively protect the heart from HF [42]. BAK is an endogenous core regulator of apoptosis [43]. Salehpour *et al.* [44] reported that CoQ10 reduced apoptosis by regulating BAK and avoiding increased caspase activity. We found that the number of apoptotic cells was significantly increased in HF mice, whereas apoptosis was reduced in the HF+CoQ10 group.

The study has some limitations. First, although CoQ10 has a variety of therapeutic applications, it is not usually prescribed as a drug because of its low oral bioavailability, which can affect its efficacy. Secondly, it should be noted that the concentration of CoQ10 in cardiac tissue on mice was not detected before and after treatment, so complete absorption of CoQ10 was not proved in the study, which is also the focus of future studies.

5. Conclusions

CoQ10 can alleviate DOX-induced cardiotoxicity, as demonstrated by the downregulation of oxidative stress, fibrosis, inflammation, energy metabolism, and apoptosis markers. These findings suggest that CoQ10 can be used as a therapeutic intervention to reduce the side effects of DOX. We only evaluated control, HF, CoQ10, and HF+CoQ10 groups and did not examine different doses of CoQ10. In addition, we did not validate cultured cells.

Author Contributions

SL and ZP designed the research study. YL, QY, and WY performed the research. LM and JY provided help and advice on immunofluorescence staining. SL and ZP analyzed the data. WY and LM wrote the manuscript. All authors contributed to editorial changes in the manuscript. All authors read and approved the final manuscript.

Ethics Approval and Consent to Participate

All animal experiments were performed in accordance with the Guide for the Care and Use of Laboratory Animals and approved by the Ethics Committee of Dalian Municipal Central Hospital.

Acknowledgment

Not applicable.

Funding

This study was funded by the Beijing Jiekai Cardiovascular Health Foundation [grant number BW20220302].

Conflict of Interest

The authors declare no conflict of interest.

References

- [1] Heidenreich PA, Bozkurt B, Aguilar D, Allen LA, Byun JJ, Colvin MM, *et al.* 2022 AHA/ACC/HFSA Guideline for the Management of Heart Failure: A Report of the American College of Cardiology/American Heart Association Joint Committee on Clinical Practice Guidelines. *Circulation*. 2022; 145: e895–e1032.
- [2] Truby LK, Rogers JG. Advanced Heart Failure: Epidemiology, Diagnosis, and Therapeutic Approaches. *JACC: Heart Failure*. 2020; 8: 523–536.
- [3] Herrmann J, Lerman A, Sandhu NP, Villarraga HR, Mulvagh SL, Kohli M. Evaluation and Management of Patients with Heart Disease and Cancer: Cardio-Oncology. *Mayo Clinic Proceedings*. 2014; 89: 1287–1306.
- [4] Tang L, Jiang W, Wu L, Yu X, He Z, Shan W, *et al.* TPGS2000-DOX Prodrug Micelles for Improving Breast Cancer Therapy. *International Journal of Nanomedicine*. 2021; 16: 7875–7890.
- [5] Xu J, Liu D, Niu H, Zhu G, Xu Y, Ye D, *et al.* Resveratrol reverses Doxorubicin resistance by inhibiting epithelial-mesenchymal transition (EMT) through modulating PTEN/Akt signaling pathway in gastric cancer. *Journal of Experimental & Clinical Cancer Research*. 2017; 36: 19.
- [6] Chung W, Youn H. Pathophysiology and preventive strategies of anthracycline-induced cardiotoxicity. *The Korean Journal of Internal Medicine*. 2016; 31: 625–633.
- [7] Breckenridge R. Heart failure and mouse models. *Disease Models & Mechanisms*. 2010; 3: 138–143.
- [8] Shabalala S, Muller CJF, Louw J, Johnson R. Polyphenols, autophagy and doxorubicin-induced cardiotoxicity. *Life Sciences*. 2017; 180: 160–170.
- [9] Koleini N, Kardami E. Autophagy and mitophagy in the context of doxorubicin-induced cardiotoxicity. *Oncotarget*. 2017; 8: 46663–46680.
- [10] Shukla S, Dubey KK. CoQ10 a super-vitamin: review on application and biosynthesis. *3 Biotech*. 2018; 8: 249.
- [11] Gati S, Camm CF. European Heart Journal-Case Report Educational Training Programme. *European Heart Journal*. 2021; 5: ytab070.
- [12] Testai L, Martelli A, Flori L, Cicero AFG, Colletti A. Coenzyme Q10: Clinical Applications beyond Cardiovascular Diseases. *Nutrients*. 2021; 13: 1697.
- [13] Raizner AE. Coenzyme Q10. *Methodist DeBakey Cardiovascular Journal*. 2019; 15: 185–191.
- [14] Jafari M, Mousavi SM, Asgharzadeh A, Yazdani N. Coenzyme Q10 in the treatment of heart failure: a systematic review of systematic reviews. *Indian Heart Journal*. 2018; 70: S111–S117.
- [15] Khan NA, Abid M, Ahmad A, Abuzinadah MF, Basheikh M, Kishore K. Cardioprotective Effect of Coenzyme Q10 on Apoptotic Myocardial Cell Death by Regulation of Bcl-2 Gene Expression. *Journal of Pharmacology and Pharmacotherapeutics*. 2017; 8: 122–127.
- [16] Zhang X, Liu H, Hao Y, Xu L, Zhang T, Liu Y, *et al.* Coenzyme Q10 protects against hyperlipidemia-induced cardiac damage in apolipoprotein E-deficient mice. *Lipids in Health and Disease*. 2018; 17: 279.
- [17] Berretta M, Quagliarillo V, Maurea N, Di Francia R, Sharifi S, Facchini G, *et al.* Multiple Effects of Ascorbic Acid against Chronic Diseases: Updated Evidence from Preclinical and Clinical Studies. *Antioxidants*. 2020; 9: 1182.
- [18] Song HS, Kim HR, Park TW, Cho BJ, Choi MY, Kim CJ, *et al.* Antioxidant Effect of CoQ10 on N-nitrosodiethylamine-induced Oxidative Stress in Mice. *The Korean Journal of Physiology and Pharmacology*. 2009; 13: 321–326.
- [19] Felker GM, Thompson RE, Hare JM, Hruban RH, Clemetson DE, Howard DL, *et al.* Underlying Causes and Long-Term Sur-

- vival in Patients with Initially Unexplained Cardiomyopathy. *New England Journal of Medicine*. 2000; 342: 1077–1084.
- [20] Angsutararux P, Luanpitpong S, Issaragrisil S. Chemotherapy-Induced Cardiotoxicity: Overview of the Roles of Oxidative Stress. *Oxidative Medicine and Cellular Longevity*. 2015; 2015: 795602.
- [21] Tadokoro T, Ikeda M, Ide T, Deguchi H, Ikeda S, Okabe K, *et al.* Mitochondria-dependent ferroptosis plays a pivotal role in doxorubicin cardiotoxicity. *JCI Insight*. 2020; 5: e132747.
- [22] Meng L, Lin H, Zhang J, Lin N, Sun Z, Gao F, *et al.* Doxorubicin induces cardiomyocyte pyroptosis via the TINCRC-mediated posttranscriptional stabilization of NLR family pyrin domain containing 3. *Journal of Molecular and Cellular Cardiology*. 2019; 136: 15–26.
- [23] Zhao L, Zhang B. Doxorubicin induces cardiotoxicity through upregulation of death receptors mediated apoptosis in cardiomyocytes. *Scientific Reports*. 2017; 7: 44735.
- [24] Li D, Yang Y, Wang S, He X, Liu M, Bai B, *et al.* Role of acetylation in doxorubicin-induced cardiotoxicity. *Redox Biology*. 2021; 46: 102089.
- [25] Tabrizi R, Akbari M, Sharifi N, Lankarani KB, Moosazadeh M, Kolahdooz F, *et al.* The Effects of Coenzyme Q10 Supplementation on Blood Pressures among Patients with Metabolic Diseases: a Systematic Review and Meta-analysis of Randomized Controlled Trials. *High Blood Pressure & Cardiovascular Prevention*. 2018; 25: 41–50.
- [26] Gutierrez-Mariscal FM, Yubero-Serrano EM, Villalba JM, Lopez-Miranda J. Coenzyme Q10: From bench to clinic in aging diseases, a translational review. *Critical Reviews in Food Science and Nutrition*. 2019; 59: 2240–2257.
- [27] Di Lorenzo A, Iannuzzo G, Parlato A, Cuomo G, Testa C, Coppola M, *et al.* Clinical Evidence for Q10 Coenzyme Supplementation in Heart Failure: From Energetics to Functional Improvement. *Journal of Clinical Medicine*. 2020; 9: 1266.
- [28] Rossi P, Diffrancia R, Quagliarriello V, Savino E, Tralongo P, Randazzo CL, *et al.* B-glucans from *Grifola frondosa* and *Ganoderma lucidum* in breast cancer: an example of complementary and integrative medicine. *Oncotarget*. 2018; 9: 24837–24856.
- [29] Iwase S, Kawaguchi T, Yotsumoto D, Doi T, Miyara K, Odagiri H, *et al.* Efficacy and safety of an amino acid jelly containing coenzyme Q10 and l-carnitine in controlling fatigue in breast cancer patients receiving chemotherapy: a multi-institutional, randomized, exploratory trial (JORTC-CAM01). *Supportive Care in Cancer*. 2016; 24: 637–646.
- [30] van der Pol A, van Gilst WH, Voors AA, van der Meer P. Treating oxidative stress in heart failure: past, present and future. *European Journal of Heart Failure*. 2019; 21: 425–435.
- [31] Cappetta D, De Angelis A, Sapio L, Prezioso L, Illiano M, Quaini F, *et al.* Oxidative Stress and Cellular Response to Doxorubicin: a Common Factor in the Complex Milieu of Anthracycline Cardiotoxicity. *Oxidative Medicine and Cellular Longevity*. 2017; 2017: 1521020.
- [32] Kitada M, Ogura Y, Monno I, Koya D. Sirtuins and Type 2 Diabetes: Role in Inflammation, Oxidative Stress, and Mitochondrial Function. *Frontiers in Endocrinology*. 2019; 10: 187.
- [33] Jin Y, Gu W, Chen W. Sirt3 is critical for p53-mediated ferroptosis upon ROS-induced stress. *Journal of Molecular Cell Biology*. 2021; 13: 151–154.
- [34] Jiang Y, Liu Y, Xiao W, Zhang D, Liu X, Xiao H, *et al.* Xinmailong Attenuates Doxorubicin-Induced Lysosomal Dysfunction and Oxidative Stress in H9c2 Cells via HO-1. *Oxidative Medicine and Cellular Longevity*. 2021; 2021: 5896931.
- [35] Dłudla PV, Orlando P, Silvestri S, Marcheggiani F, Cirilli I, Nyambuya TM, *et al.* Coenzyme Q (10) Supplementation Improves Adipokine Levels and Alleviates Inflammation and Lipid Peroxidation in Conditions of Metabolic Syndrome: A Meta-Analysis of Randomized Controlled Trials. *International Journal of Molecular Sciences*. 2020; 21: 3247.
- [36] Harris GS, Lust RM, DeAntonio JH, Katwa LC. PPAR-gamma expression in animals subjected to volume overload and chronic Urotensin II administration. *Peptides*. 2008; 29: 795–800.
- [37] Nair AR, Agbor LN, Mukohda M, Liu X, Hu C, Wu J, *et al.* Interference with Endothelial PPAR (Peroxisome Proliferator-Activated Receptor)- γ Causes Accelerated Cerebral Vascular Dysfunction in Response to Endogenous Renin-Angiotensin System Activation. *Hypertension*. 2018; 72: 1227–1235.
- [38] Quagliarriello V, Vecchione R, De Capua A, Lagreca E, Iaffaioli RV, Botti G, *et al.* Nano-Encapsulation of Coenzyme Q10 in Secondary and Tertiary Nano-Emulsions for Enhanced Cardioprotection and Hepatoprotection in Human Cardiomyocytes and Hepatocytes During Exposure to Anthracyclines and Trastuzumab. *International Journal of Nanomedicine*. 2020; 15: 4859–4876.
- [39] Palomo J, Dietrich D, Martin P, Palmer G, Gabay C. The interleukin (IL)-1 cytokine family – Balance between agonists and antagonists in inflammatory diseases. *Cytokine*. 2015; 76: 25–37.
- [40] S Yousef AO, A Fahad A, Abdel Moneim AE, Metwally DM, El-Khadragy MF, Kassab RB. The Neuroprotective Role of Coenzyme Q10 Against Lead Acetate-Induced Neurotoxicity Is Mediated by Antioxidant, Anti-Inflammatory and Anti-Apoptotic Activities. *International Journal of Environmental Research and Public Health*. 2019; 16: 2895.
- [41] Sugizaki T, Tanaka K, Asano T, Kobayashi D, Hino Y, Takafuji A, *et al.* Idebenone has preventative and therapeutic effects on pulmonary fibrosis via preferential suppression of fibroblast activity. *Cell Death Discovery*. 2019; 5: 146.
- [42] Deng H, Ouyang W, Zhang L, Xiao X, Huang Z, Zhu W. LncRNA GASL1 is downregulated in chronic heart failure and regulates cardiomyocyte apoptosis. *Cellular & Molecular Biology Letters*. 2019; 24: 41.
- [43] Peña-Blanco A, García-Sáez AJ. Bax, Bak and beyond — mitochondrial performance in apoptosis. *The FEBS Journal*. 2018; 285: 416–431.
- [44] Salehpour F, Farajdokht F, Cassano P, Sadigh-Eteghad S, Erfani M, Hamblin MR, *et al.* Near-infrared photobiomodulation combined with coenzyme Q (10) for depression in a mouse model of restraint stress: reduction in oxidative stress, neuroinflammation, and apoptosis. *Brain Research Bulletin*. 2019; 144: 213–222.